Biogeosciences Discuss., 9, 387–409, 2012
www.biogeosciences-discuss.net/9/387/2012/
doi:10.5194/bgd-9-387-2012
© Author(s) 2012. CC Attribution 3.0 License.

Biogeosciences Discussions

This discussion paper is/has been under review for the journal Biogeosciences (BG).
Please refer to the corresponding final paper in BG if available.

Seasonal Variability of Tropical Wetland CH_4 emissions: the role of the methanogen-available carbon pool

A. A. Bloom, P. I. Palmer, A. Fraser, and D. S. Reay

School of GeoSciences, University of Edinburgh, Edinburgh, UK

Received: 21 November 2011 – Accepted: 12 December 2011 – Published: 12 January 2012

Correspondence to: A. A. Bloom (a.a.bloom@ed.ac.uk)

Published by Copernicus Publications on behalf of the European Geosciences Union.

Abstract

We develop a dynamic methanogen-available carbon model (DMCM) to quantify the role of the methanogen-available carbon pool in determining the spatial and temporal variability of tropical wetland CH_4 emissions over seasonal timescales. We fit DMCM parameters to satellite observations of CH_4 columns from SCIAMACHY CH_4 and equivalent water height (EWH) from GRACE. Over the Amazon river basin we find substantial seasonal variability of this carbon pool (coefficient of variation = 28 ± 22 %) and a rapid decay constant ($\phi = 0.017\,day^{-1}$), in agreement with available laboratory measurements, suggesting that plant litter is likely the prominent methanogen carbon source over this region. Using the DMCM we derive global CH_4 emissions for 2003–2009, and determine the resulting seasonal variability of atmospheric CH_4 on a global scale using the GEOS-Chem atmospheric chemistry and transport model. First, we estimate tropical emissions amount to $111.1\,Tg\,CH_4\,yr^{-1}$ of which 24 % is emitted from Amazon wetlands. We estimate that annual tropical wetland emissions have increased by $3.4\,Tg\,CH_4\,yr^{-1}$ between 2003 and 2009. Second, we find that the model is able to reproduce the observed seasonal lag between CH_4 concentrations peaking 1–3 months before peak EWH values. We also find that our estimates of CH_4 emissions substantially improve the comparison between the model and observed CH_4 surface concentrations ($r = 0.9$). We anticipate that these new insights from the DMCM represent a fundamental step in parameterising tropical wetland CH_4 emissions and quantifying the seasonal variability and future trends of tropical CH_4 emissions.

1 Introduction

Wetlands are the single largest source of methane (CH_4) into the atmosphere and account for 20–40 % of the global CH_4 source (Denman et al., 2007), of which tropical wetlands account for 50–60 % of this global wetland CH_4 source (e.g. Cao et al., 1996; Bloom et al., 2010). Tropical wetland biogeochemistry is poorly understood compared

BGD
9, 387–409, 2012

to boreal peatlands (Mitsch et al., 2010), resulting in large inter-model discrepancies of the magnitude and distribution of tropical wetland CH_4 emission estimates (Riley et al., 2011). Tropical climate variability (e.g., resulting in widespread droughts, Lewis et al., 2011) can lead to large year to year variations in tropical wetland CH_4 emissions and subsequently the global CH_4 budget (Hodson et al., 2011). An improved quantitative understanding of the magnitude, distribution, and variation of tropical wetland CH_4 emissions is therefore essential to further understanding of the global CH_4 cycle. Here, we parameterise tropical wetland CH_4 emissions, and hence introduce a predictive capability that can be used to determine future emissions and to help quantify global CH_4 climate feedbacks.

In wetlands and rice paddies, methanogenesis (the biogenic production of CH_4) occurs as the final step of anoxic organic matter decomposition (Neue et al., 1997). Factors influencing methanogenesis rates include substrate availability, soil pH, temperature, water table position and redox potential (Whalen, 2005). Wetland vegetation type and aquatic herbivore activity can also affect the transport of CH_4 between the soil and atmosphere (Joabsson et al., 1999; Dingemans et al., 2011). On a global scale, seasonal variations in wetland CH_4 fluxes are mostly determined by temporal changes in wetland water volume and soil temperature (Walter et al., 2001; Gedney et al., 2004), and from seasonal changes in wetland extent and wetland water table depth (Ringeval et al., 2010; Bloom et al., 2010). Recent work that used SCIAMACHY lower tropospheric CH_4 column concentrations and Gravity Recovery And Climate Experiment (GRACE) equivalent water height (EWH) retrievals shows that the seasonality of wetland CH_4 emissions can be largely explained by seasonal changes in surface temperature and water volume (Bloom et al., 2010). The Amazon and Congo river basins were the only major exceptions in this study, where CH_4 concentrations peaked several weeks before EWH, highlighting our incomplete understanding of the processes controlling tropical wetland CH_4 emissions over seasonal timescales.

In this paper we focus on the seasonal lag between CH_4 emissions and flooding over the Amazon river basin area (Oki and Sud, 1998). We use SCIAMACHY CH_4 retrievals

BGD
9, 387–409, 2012

and GRACE EWH (both described in Sect. 2.2) to determine the seasonal lag between wetland CH_4 emissions and wetland water volume. Figure 1 shows that seasonal flooding of the Amazon basin occurs typically 1–3 months after the peak CH_4 concentrations, and to a lesser extent the lag persists throughout tropical wetland areas. In Sect. 2, we test the hypothesis that this lag is related to the depletion of methanogen-available carbon during the onset of the tropical wet season by explicitly accounting for this carbon pool in a parameterised model of tropical wetland CH_4 emissions (Bloom et al., 2010). We optimise model parameters by fitting them to SCIAMACHY CH_4 column and GRACE EWH measurements, and use the resulting model to estimate global wetland emission estimates. In Sect. 3 we compare our results to previous estimates of wetland CH_4 emissions and to decomposition rates of methanogen-available carbon in anaerobic environments. Finally, we use our estimated emissions to drive the GEOS-Chem atmospheric chemistry model as an approach to test the consistency between our emission estimates and observed variations of atmospheric CH_4 concentration. We conclude the paper in Sect. 4.

2 Process-based model and application

Here, we introduce a methanogen-available carbon pool (C_μ) that typically originates from labile plant litter, recalcitrant organic matter decomposition and root exudates (e.g. Wania et al., 2010). Typically soil carbon pool decay constants are more than an order of magnitude lower than those of leaf litter (Sitch et al., 2003; Wania et al., 2010). Therefore, if C_μ originates mostly from the slow-decomposing recalcitrant carbon pool, then variations in C_μ over seasonal timescales are likely to be small. Conversely, if C_μ is drawn from leaf litter, then large variations in C_μ abundance may arise as a result of rapid litter decomposition in the tropics. Miyajima et al. (1997) measured CH_4 accumulation of anaerobic decomposition of incubated tropical withered tree leaves over a 200 day period. These observations show a rapid decrease in decomposition rates over the incubation period. Bianchini Jr. et al. (2010) found similar results from

BGD
9, 387–409, 2012

dried and ground anaerobic decomposition of *Oxycaryum cubense* at 20°C: following a 20-day lag (where no emissions were observed) CH_4 produced from organic carbon decomposition peaked after a 50-day period, and then rapidly decreased. On a tropical river-basin scale, flooded areas expand at the onset of the wet season and engulf newly available plant litter: as a result, CH_4 emissions from plant litter may peak before the height of the water table. The occurrence of anaerobic CH_4 emissions from litter decomposition within sub-seasonal timescales raises the question as to whether C_μ significantly varies in time.

2.1 Model description

We base our model on previous work (Bloom et al., 2010) that describes the temporal variability of wetland emissions $F^t_{CH_4}$ (mg CH_4 m^{-2} day^{-1}) as a function of EWH and surface temperature:

$$F^t_{CH_4} = k(\Gamma^t_w + D_\alpha)Q_{10}(T^t_s)^{\frac{T^t_s}{10}}, \quad (1)$$

where at time t (days), Γ^t_w is the EWH, T^t_s is the surface temperature (K), D_α is the equivalent depth of the wetland soil (m), $Q_{10}(T^t_s)$ is the temperature dependence function implemented by Gedney et al. (2004), and k is a scaling constant (mg CH_4 m^{-2} day^{-1}) accounting for all temporally constant factors (e.g. Gedney et al., 2004).

Equation (1) assumes an inexhaustible source of methanogen-available carbon. Here we account for the potential seasonal changes in C_μ by substituting k with $\phi_0 C^t_\mu$, where ϕ_0 (day^{-1}) is the temperature, water and carbon independent decay constant of wetland methanogenesis, and C^t_μ is the value of C_μ (mg CH_4 m^{-2}) at time t:

$$F^t_{CH_4} = \phi_0 C^t_\mu(\Gamma^t_w + D_\alpha)Q_{10}(T_s)^{\frac{T^t_s}{10}}. \quad (2)$$

BGD
9, 387–409, 2012

To determine temporal changes in C_μ, we define C_μ^{t+1} in terms of C_μ^t:

$$C_\mu^{t+1} = C_\mu^t + N_\mu \Delta t - F_{CH_4}^t \Delta t, \quad (3)$$

where Δt is the time interval, $F_{\mathrm{CH}_4}^t$ is the carbon loss due to emitted CH_4 (Eq. 2), N_μ is the net influx of carbon available for methanogenesis from plant litter, root exudates, and breakdown of complex polymers from the recalcitrant carbon pool. We assume N_μ is temporally constant, and we assume wetland carbon stocks are in quasi-equilibrium on annual timescales, hence $\overline{N_\mu} = \overline{F_{\mathrm{CH}_4}^t}$. Note that when ϕ_0 is small, the equilibrium $C_\mu \gg N_\mu \Delta t$. In this case, $C_\mu^{t+1} \simeq C_\mu^t$ and Eq. (2) converges to Eq. (1) (Bloom et al., 2010), which assumes $\phi_0 C_\mu$ is constant over seasonal timescales. In order to compare derived decay constants with observed and model values (e.g. Miyajima et al., 1997; Wania et al., 2010), we determine the annual mean decay constant of wetlands areas as $\overline{\phi} = \overline{F_{\mathrm{CH}_4}^t} / \overline{C_\mu^t}$ (day^{-1}). Equations (2) and (3) constitute the dynamic methanogen-available carbon model (DMCM).

2.2 Data

For the sake of brevity we only include a brief description of the datasets for our analysis and refer the reader to dedicated papers. Solar backscatter data from the Scanning Imaging Absorption Spectrometer for Atmospheric Cartography (SCIAMACHY) instrument onboard Envisat is used to retrieve the mean column concentrations of CH_4 in the atmosphere (Frankenberg et al., 2005). The spatial resolution of CH_4 retrievals is 30 km × 60 km, and the Envisat orbital geometry ensures global coverage at 6-day intervals. CH_4 retrievals are only achievable in daytime cloud-free conditions. The Gravity Recovery and Climate Experiment (GRACE) is a twin satellite system from which the Earth's gravity field is retrieved at 10-day intervals. Tides, atmospheric pressure and wind are included in the applied corrections on GRACE gravity retrievals: the remaining temporal variation in GRACE gravity is dominated by terrestrial water variability

BGD
9, 387–409, 2012

(Tapley et al., 2004). We incorporate SCIAMACHY CH_4 concentrations, GRACE EWH and NCEP/NCAR daily 1.9°× 1.88° temperature re-analyses (Kalnay et al., 1996) into a process-based model following Bloom et al. (2010). We use the 2003–2008 SCIAMACHY column CH_4 retrievals (Frankenberg et al., 2008), and the CNES GRACE EWH 1°×1° 10-day resolution product (Lemoine et al., 2007): we aggregate all three datasets to a daily 3°×3° horizontal grid (see Bloom et al., 2010).

2.3 Global parameter optimisation

We implement the DMCM on a global 3° × 3° grid for the period 2003–2009. We drive the DMCM using the aggregated daily values of T_s^t and Γ_w^t. We spin up the DMCM using 2003 T_s^t and Γ_w^t values until it reaches an annual equilibrium ($\overline{N_\mu} = \overline{F_{CH_4}^t}$). In contrast to Bloom et al. (2010), we supplement the $Q_{10}(T_s)$ function with a gradual linear cut-off for temperatures for 0°C $< T_s^t <$ −10°C, and when $T_s^t <$ −10°C, $F_{CH_4}^t = 0$ as a first order approximation to wintertime CH_4 emission inhibition in boreal wetlands. As the Q_{10} function never reaches zero, this supplementary constraint will effectively suppress winter-time CH_4 emissions, which is broadly consistent with our current understanding of CH_4 emissions in boreal wetlands.

We apply the DMCM globally in order to determine (i) the magnitude of $\overline{\phi}$ and C_μ in the tropics within each 3° × 3° gridcell (ii) the potential of C_μ temporal variability on extra-tropical wetland environments, and (iii) CH_4 emissions from wetlands and rice paddies at a global scale. We determine the global distribution and seasonal variability of wetland CH_4 emissions by optimising parameters ϕ_0 and D_α at each gridcell by minimising the following cost function (J):

$$J = \sum_{t=1}^{n} (\kappa * \Delta F_{CH_4}^t - \Delta S_{CH_4}^t)^2, \quad (4)$$

BGD
9, 387–409, 2012

where $\Delta S^t_{CH_4}$ denotes the SCIAMACHY CH_4 variability after we remove the interannual trend (represented as a 2nd order polynomial); $F^t_{CH_4}$ is derived from Eqs. (2) and (3); and the conversion factor κ (ppm kg^{-1} CH_4 m^{-2} day^{-1}) relates CH_4 emissions to the equivalent column concentration in the lower troposphere (e.g. Bloom et al., 2010). We then implement the global $Q_{10}(T_s)$ optimisation approach of Bloom et al. (2010). Like other top-down parameter optimisation methods of global wetland CH_4 emissions (Gedney et al., 2004; Bloom et al., 2010), our method is unable to distinguish between the seasonality of CH_4 emissions from wetlands and rice paddies due to the concurring fluxes over seasonal timescales, although we anticipate varying fertilisation and irrigation practices will also influence the seasonality in rice paddy CH_4 emissions (Conen et al., 2010). We hence distinguish the sources spatially (Bloom et al., 2010) for which we have more confidence in the distribution of rice paddies. Finally, we use the IPCC global wetland and rice paddy CH_4 emissions median of 227.5 Tg CH_4 yr^{-1} (Denman et al., 2007) as a base value for 2003 emissions.

We propagate the following uncertainties through our global wetland and rice paddy CH_4 emissions estimation (Bloom et al., 2010): (i) SCIAMACHY CH_4 observation errors; (ii) the uncertainty of the linear fit between $F^t_{CH_4}$ and $S^t_{CH_4}$; (iii) the uncertainty $\sigma_\kappa = \pm 16\,\%$ associated with κ; and (iv) a global wetland and rice paddy uncertainty of $\pm$ 58 Tg CH_4 yr^{-1} (Denman et al., 2007).

3 Results and discussion

Over the Amazon river basin we find wetland CH_4 fluxes coinciding with small values of C_μ, resulting in a highly variable C_μ over seasonal timescales. Assuming an annual mean inundated fraction of 3.3 % (Prigent et al., 2007), the median CH_4 flux over a flooded area is 1.06 Mg C ha^{-1} (369 mg CH_4 m^{-2} day^{-1}). The median Amazon wetland C_μ = 0.16 Mg C ha^{-1} with a range of 0.02–7.89 Mg C ha^{-1} (5th–95th percentile). The large spatial variability of C_μ is consistent with the complexity of methanogenesis rates

BGD
9, 387–409, 2012

in wetlands (Neue et al., 1997; Whalen, 2005). Large temporal changes of C_μ are observed in the Amazon river basin where the mean C_μ coefficient of variation (c_v) is 28 ± 22 % over the period 2003–2009. When we allow C_μ to vary in extra-tropical regions we find a median of $c_v < 0.1$ %, and as a result the relatively small C_μ variability does not influence the seasonality of CH_4 emissions outside the tropics. For rice paddy areas in southeast Asia we find a median of $c_v = 4.8$ %. We acknowledge that due to the varying rice cultivation practices around the world (Conen et al., 2010), the effects of rice paddy irrigation and the timing of fertilisation on C_μ cannot be captured by the DMCM approach.

To determine whether our derived values for C_μ and $\overline{\phi}$ are relevant to tropical ecosystems, we compare them against laboratory measurements of anaerobic decomposition of withered leaves from a wetland region in Narathiwat, Thailand (Miyajima et al., 1997). We simulate CH_4 production from C_μ at each model gridcell for a 200-day period without fresh carbon input (N_μ=0), and we use innundated fraction observations (Prigent et al., 2007) to determine the flux magnitude over flooded areas only. Figure 2 shows the cumulative CH_4 production over a 200-day period for (i) simulated decomposition from derived $\overline{\phi}$ and C_μ values over the Amazon, (ii) simulated decomposition from derived $\overline{\phi}$ and C_μ values over boreal wetlands, and (iii) upscaled withered leaf mineralisation rates by Miyajima et al. (1997) using a median of 17.5 Mg C ha^{-1} fine and coarse woody debris (Malhi et al., 2009). For boreal and tropical C_μ decomposition, the median cumulative CH_4 emissions, 68 % confidence interval, and mean decay constants ($\overline{\phi}$) are shown. For the withered leaf mineralisation rates, we show the mean fitted decay constant ($\overline{\phi}$) and the range and median cumulative CH_4 emissions.

The top-down parameter estimation of $\overline{\phi}$ and C_μ suggest plant litter C_μ is a fundamental component of tropical CH_4 emission seasonality. Our top-down estimation of anaerobic decomposition rates for tropical wetland CH_4 emissions compare favourably with laboratory measurements of anaerobically produced CH_4: while the magnitude of tropical C_μ decomposition is more than a factor of two smaller than laboratory

BGD
9, 387–409, 2012

measurements (Miyajima et al., 1997), the mean decay constant $\overline{\phi}_{\text{Amazon}} = 0.017\,\text{day}^{-1}$ compares well to $\overline{\phi}_{\text{leaf}} = 0.011\,\text{day}^{-1}$ for withered leaf decomposition. The larger laboratory measurements (Miyajima et al., 1997) are partially explained by an incubation temperature of 35 °C (cf. a mean surface temperature in the Amazon basin of 23 °C), and the lack of observations for coarse woody debris decomposition. As a result of relatively high $\overline{\phi}$ values, measured leaf decomposition and model CH_4 emissions both show a significant reduction of CH_4 emission rates throughout the 200-day period. In contrast, the boreal decay constant ($\overline{\phi}_{\text{Boreal}} = 0.0003\,\text{day}^{-1}$) indicates relatively constant CH_4 emission rates throughout the 200-day period.

Table 1 shows a comparison between observed and model decay constants derived from a variety of methods. The range of $\overline{\phi}_{\text{Amazon}}$ values are within the order of magnitude of leaf and wetland macrophyte decay constants (Miyajima et al., 1997; Longhi et al., 2008; Wania et al., 2010). We believe that $\overline{\phi}_{\text{Amazon}}$ is an indicator for the cumulative decay constant of the rapid anaerobic decomposition of root exudates, plant litter decomposition, and the contribution of recalcitrant carbon pools. For a more detailed $\overline{\phi}_{\text{Amazon}}$ comparison with observed and model decay constant values, an estimation of the overall $\overline{\phi}$ in wetland CH_4 production from bottom-up process-based models (e.g. Wania et al., 2010) is needed.

Figure 3 shows the total CH_4 flux over the central branch of the Amazon river (0° N–6° S, 80° W–40° W). The temporal changes in C_μ result in a significantly different timing for CH_4 emissions over the tropics in comparison to the Bloom et al. (2010) water volume and temperature dependence approach. While in the dry season the minimum CH_4 fluxes coincide with the lowest GRACE EWH, peak CH_4 fluxes occur during the rising water phase. The DMCM optimisation predicts that the accumulation of carbon in the dry season results in higher C_μ values at the onset of the wet season. This carbon pool is then rapidly depleted during the wet season. As a result, CH_4 emission rates begin to decrease before the peak water phase in the wet season. CH_4 oxidation within the water column has been proposed as a mechanism explaining reduced CH_4

BGD
9, 387–409, 2012

emissions during the peak of the wet season (Mitsch et al., 2010), although this would result in a second CH_4 peak at the end of the wet season. The absence of this peak in our analysis suggests this process plays only a minor role in the seasonality of tropical wetland CH_4 emissions.

By globally integrating the DMCM method we estimated tropical wetlands emit 111.1 Tg CH_4 yr^{-1}, where Amazon wetlands account for 26.2 Tg CH_4 yr^{-1} (24 %). Table 2 shows our estimates are within the range of other independent Amazon wetland emission CH_4 estimates. Figure 4 shows the zonal profile of our top-down approach with the associated uncertainty estimates. We capture three main features of global wetland and rice paddy emissions, i.e. peaks over the tropics, subtropics and lower mid-latitudes (mainly due to rice), and boreal latitudes, in agreement with previous studies (Bloom et al., 2010; Fung et al., 1991; Riley et al., 2011). In comparison to our previous work (Bloom et al., 2010) we find a slight reduction in boreal wetland emissions (3.2 %), primarily due to the introduction of a gradual cut-off in methanogenesis rates under 0°C (Sect. 2.3). During 2003–2008, the global change in CH_4 wetland emissions amounts to an increase of 7.7 Tg CH_4 yr^{-1}, mostly as a result of boreal wetlands (3.1 Tg CH_4 yr^{-1}) and tropical wetlands (3.4 Tg CH_4 yr^{-1}), while there is also a significant increase of 1.1 Tg CH_4 yr^{-1} from mid-latitude wetlands. The increase in Southern Hemisphere extra-tropical wetland emissions (0.13 Tg CH_4 yr^{-1}) did not significantly contribute to the CH_4 wetland emissions growth during 2003–2008.

Finally, we use our wetland and rice CH_4 emission estimates to drive the GEOS-Chem global 3-D atmospheric chemistry and transport model (described and evaluated by Fraser et al., 2011) allowing us to test consistency between our emissions to surface measurements of CH_4 concentrations. We sample the model at the time and geographical location of the surface CH_4 measurements from the GasLab, AGAGE and ESRL networks (Francey et al., 1996; Prinn et al., 2000; Cunnold et al., 2002; Dlugokencky et al., 2009). Figure 5 shows model and observed CH_4 concentration anomalies (i.e., minus the mean trend) for the northern and Southern Hemispheres. We chose to remove the interannual trend from all CH_4 concentrations to compare the

BGD
9, 387–409, 2012

seasonality of model and surface measurements of CH_4. We show that the DMCM approach better describes the observed seasonality in both hemispheres ($r_{NH} = 0.9$, $r_{SH} = 0.9$), and the amplitude of the Southern Hemisphere seasonality is largely improved in comparison to the GEOS-Chem runs using Fung et al. (1991) and Bloom et al. (2010) CH_4 emissions.

4 Concluding remarks

Understanding the temporal controls of temperature, water volume and carbon content of wetlands is crucial in determining the global and regional seasonal cycle of wetland CH_4 emissions. We show that incorporating a temporally variable methanogen-available carbon pool, C_μ, in our top-down approach results in a significant improvement in describing the temporal behaviour of tropical and global CH_4 emissions.

By implementing our dynamic methanogen-available carbon model (DMCM) on a global scale we determine the effects of a seasonally variable C_μ on the seasonality of wetland CH_4 emissions in the Amazon river basin. We find a median decay constant of $\overline{\phi}_{Amazon} = 0.017\,day^{-1}$ over the Amazon river basin. Seasonal changes in C_μ in the tropics largely explain the seasonal lag between SCIAMACHY observed CH_4 concentrations and GRACE equivalent water height. The relatively high seasonal variability in C_μ (mean $c_v = 28\,\%$) over the Amazon river basin results in peak CH_4 emissions occurring mostly 1–3 months prior to the peak water height period: in contrast, the median boreal C_μ variability is $c_v < 0.1\,\%$. We show a substantial improvement in simulating surface concentrations when using the GEOS-Chem ACTM with our wetland and rice CH_4 emission estimates ($r = 0.9$). These improvements in the magnitude and temporal dynamics of tropical CH_4 emissions will ultimately help constrain global inverse modelling efforts.

We anticipate that this work will lead to further and more detailed parameterisation of tropical wetland CH_4 emissions, and we expect our tropical wetland CH_4 emission parameterisation will reduce the uncertainty in forecasting future changes in wetland CH_4 emissions.

BGD
9, 387–409, 2012

Acknowledgements. We thank Catherine Prigent for providing global inundated fraction data and Christian Frankenberg for providing the SCIAMACHY CH4 retrievals. We thank Nancy Burns for her input on model and measured decomposition rate comparison. The surface measurements were provided by the NASA AGAGE network, the NOAA ESRL network, and the CSIRO Marine and Atmospheric Research GASLab network. A. A. B. was supported by the UK Natural Environmental Research Council (NERC) studentship NE F007973 1 and funds from P. I. P.'s Philip Leverhulme Prize. A. F. was supported by the NERC National Centre for Earth Observation.

References

Bianchini Jr., I., Cunha-Santino, M. B. d., Romeiro, F., and Bitar, A. L.: Emissions of methane and carbon dioxide during anaerobic decomposition of aquatic macrophytes from a tropical lagoon (São Paulo, Brazil), Acta Limnologica Brasiliensia, 22, 157–164, 2010. 390

Bloom, A. A., Palmer, P. I., Fraser, A., Reay, D. S., and Frankenberg, C.: Large-Scale Controls of Methanogenesis Inferred from Methane and Gravity Spaceborne Data, Science, 327, 322–325, 2010. 388, 389, 390, 391, 392, 393, 394, 396, 397, 398, 404, 408, 409

Cao, M., Marshall, S., and Gregso, K.: Global carbon exchange and methane emissions from natural wetlands: Application of a process-based model, J. Geophys. Res., 101, 14399–14414, 1996. 388

Conen, F., Smith, K. A., and Yagi, K.: Methane from rice cultivation, in: Methane and Climate Change, edited by: Reay, D., Smith, P., and van Amstel, A., Earthscan, London, UK, 115–135, iSBN 9781844078233, 2010. 394, 395

Cunnold, D. M., Steele, L. P., Fraser, P. J., Simmonds, P. G., Prinn, R. G., Weiss, R. F., Porter, L. W., O'Doherty, S., Langenfelds, R. L., Krummel, P. B., Wang, H. J., Emmons, L., Tie, X. X., and Dlugokencky, E. J.: In situ measurements of atmospheric methane at GAGE/AGAGE sites during 1985-2000 and resulting source inferences, J. Geophys. Res. Atmos., 107, 4225, doi:10.1029/2001JD001226, 2002. 397, 409

Denman, K., Brasseur, G., Chidthaisong, A., Ciai, P., Cox, P., Dickinson, R., Hauglustaine, D., Heinze, C., Holland, E., Jacob, D., Lohmann, U., Ramachandran, S., da Silva Dias, P., Wofsy, S., and Zhang, X.: Couplings Between Changes in the Climate System and Biogeochemistry, in: Climate Change 2007: The Physical Science Basis. Contribution of Working Group I to

BGD

9, 387–409, 2012

the Fourth Assessment Report of the Intergovernmental Panel on Climate Change edited by: Solomon, S., Qin, D., Manning, M., Chen, Z., Marquis, M., Averyt, K. B., Tignor, M., and Miller, H. L., Cambridge University Press, Cambridge, UK and New York, NY, USA, 2007. 388, 394

Dingemans, B., Bakker, E., and Bodelier, P.: Aquatic herbivores facilitate the emission of methane from wetlands, Ecology, 92, 1166–1173, 2011. 389

Dlugokencky, E. J., Lang, P., and Masarie, K.: Atmospheric Methane Dry Air Mole Fractions from the NOAA ESRL Carbon Cycle Cooperative Global Air Sampling Network, 1983–2007, Version: 2008-07-02, 2009. 397, 409

Francey, R. L., Steele, L., Langenfelds, R., Lucarelli, M., Allison, C., Beardsmore, D., Coram, S., Derek, N., de Silva, F., Etheridge, D., Fraser, P., Henry, R., Turner, B., Welch, E., Spencer, D., and Cooper, L.: Global Atmospheric Sampling Laboratory (GASLAB): supporting and extending the Cape Grim trace gas programs. Baseline Atmospheric Program (Australia) 1993, edited by: Francey, R. J., Dick, A. L., and Derek, N., 8–29, Bureau of Meteorology and CSIRO Division of Atmospheric Research, Melbourne, Australia, 1996. 397, 409

Frankenberg, C., Meirink, J. F., van Weele, M., Platt, U., and Wagner, T.: Assessing Methane Emissions from Global Space-Borne Observations, Science, 308, 1010–1014, 2005. 392

Frankenberg, C., Warneke, T., Butz, A., Aben, I., Hase, F., Spietz, P., and Brown, L. R.: Pressure broadening in the $2\nu_3$ band of methane and its implication on atmospheric retrievals, Atmos. Chem. Phys., 8, 5061–5075, doi:10.5194/acp-8-5061-2008, 2008. 393

Fraser, A., Chan Miller, C., Palmer, P. I., Deutscher, N. M., Jones, N. B., and Griffith, D. W. T.: The Australian methane budget: Interpreting surface and train-borne measurements using a chemistry transport model, J. Geophys. Res., 116, D20306, doi:10.1029/2011JD015964, 2011. 397, 409

Fung, I., John, J., Lerner, J., Matthews, E., Prather, M., Steele, L. P., and Fraser, P. J.: Three-dimensional model synthesis of the global methane cycle, J. Geophys. Res., 96, 13033–13065, doi:10.1029/91JD01247, 1991. 397, 398, 404, 408, 409

Gedney, N., Cox, P. M., and Huntingford, C.: Climate feedback from wetland methane emissions, Geophys. Res. Lett., 31, L20503, doi:10.1029/2004GL020919, 2004. 389, 391, 394

Hodson, E. L., Poulter, B., Zimmermann, N. E., Prigent, C., and Kaplan, J. O.: The El Niño-Southern Oscillation and wetland methane interannual variability, Geophys. Res. Lett., 38, L08810, doi:10.1029/2011GL046861, 2011. 389

Joabsson, A., Christensen, T. R., and Wallen, B.: Vascular plant controls on methane emissions

BGD
9, 387–409, 2012

from northern peatforming wetlands, Trends Ecol. Evol., 14, 385–388, 1999. 389
Kalnay, E., Kanamitsu, M., Kistler, R., Collins, W., Deaven, D., Gandin, L., Iredell, M., Saha, S., White, G., Woollen, J., Zhu, Y., Leetmaa, A., Reynolds, R., Chelliah, M., Ebisuzaki, W., Higgins, W., Janowiak, J., K.C. Mo, C. R., Wang, J., Jennec, R., and Joseph, D.: The NCEP/NCAR 40-Year Reanalysis Project, B. Am. Meteorol. Soc., 77, 437–471, 1996. 393
Lemoine, J.-M., Bruinsma, S., Loyer, S., Biancale, R., Marty, J.-C., Perosanz, F., and Balmino, G.: Temporal gravity field models inferred from GRACE data, Adv. Space Res., 39, 1620–1629, doi:10.1016/j.asr.2007.03.062, 2007. 393
Lewis, S. L., Brando, P. M., Phillips, O. L., van der Heijden, G. M. F., and Nepstad, D.: The 2010 Amazon Drought, Science, 331, 554, doi:10.1126/science.1200807, 2011. 389
Longhi, D., Bartoli, M., and Viaroli, P.: Decomposition of four macrophytes in wetland sediments: Organic matter and nutrient decay and associated benthic processes, Aquat. Bot. 89, 303–310, doi:10.1016/j.aquabot.2008.03.004, 2008. 396, 403
Malhi, Y., Aragao, L. E. O. C., Metcalfe, D. B., Paiva, R., Quesada, C. A., Almeida, S., Anderson, L., Brando, P., Chambers, J. Q., Da Costa, A. C. L., Hutyra, L. R., Oliveira, P., Patino, S., Pyle, E. H., Robertson, A. L., and Teixeira, L. M.: Comprehensive assessment of carbon productivity, allocation and storage in three Amazonian forests, Global Change Biol., 15, 1255–1274, doi:10.1111/j.1365-2486.2008.01780.x, 2009. 395, 406
Melack, J. M., Hess, L. L., Gastil, M., Forsberg, B. R., Hamilton, S. K., Lima, I. B. T., and Nova, E. M. L. M.: Regionalization of methane emissions in the Amazon basin with microwave remote sensing, Global Change Biol., 10, 530–544, 2004. 404
Mitsch, W., Nahlik, A., Wolski, P., Bernal, B., Zhang, L., and Ramberg, L.: Tropical wetlands: seasonal hydrologic pulsing, carbon sequestration, and methane emissions, Wetl. Ecol. Manage., 18, 573–586, doi:10.1007/s11273-009-9164-4, 2010. 389, 397
Miyajima, T., Wada, E., Hanba, Y. T., and Vijarnsorn, P.: Anaerobic mineralization of indigenous organic matters and methanogenesis in tropical wetland soils, Geochim. Cosmochim. Ac., 61, 3739–3751, doi:10.1016/S0016-7037(97)00189-0, 1997. 390, 392, 395, 396, 403, 406
Neue, H., Wassmann, R., Kludze, H., Bujun, W., and Lantin, R.: Factors and processes controlling methane emissions from rice fields, Nutr. Cycl. Agroecosys., 49, 111–117, 1997. 389, 395
Oki, T. and Sud, Y. C.: Design of Total Runoff Integrating Pathways (TRIP) – A global river channel network, Earth Interact., 2, 1–37, 1998. 389
Prigent, C., Papa, F., Aires, F., Rossow, W. B., and Matthews, E.: Global inundation dynamics

BGD
9, 387–409, 2012

inferred from multiple satellite observations, 1993-2000, J. Geophys. Res. Atmos., 112, D12107, doi:10.1029/2006JD007847, 2007. 394, 395, 405

Prinn, R. G., Weiss, R. F., Fraser, P. J., Simmons, P. G., Cunnold, D. N., Alyea, F. N., O'Doherty, S., Salameh, P., Miller, B. R., Huang, J., Wang, R. H. J., Hartley, D. E., Harth, C., Steele, L. P., Sturrock, G., Midgley, P. M., and McCulloch, A.: A History of Chemically and Radiatively Important Gases in Air deduced from ALE/GAGE/AGAGE, J. Geophys. Res., 105, 17751–17792, 2000. 397, 409

Riley, W. J., Subin, Z. M., Lawrence, D. M., Swenson, S. C., Torn, M. S., Meng, L., Mahowald, N. M., and Hess, P.: Barriers to predicting changes in global terrestrial methane fluxes: analyses using CLM4Me, a methane biogeochemistry model integrated in CESM, Biogeosciences, 8, 1925–1953, doi:10.5194/bg-8-1925-2011, 2011. 389, 397, 404, 408

Ringeval, B., de Noblet-Ducoudré, N., Ciais, P., Bousquet, P., Prigent, C., Papa, F., and Rossow, W. B.: An attempt to quantify the impact of changes in wetland extent on methane emissions on the seasonal and interannual time scales, Global Biogeochem. Cy., 24, GB2003, doi:10.1029/2008GB003354, 2010. 389

Sitch, S., Smith, B., Prentice, I. C., Arneth, A., Bondeau, A., Cramer, W., Kaplan, J. O., Levis, S., Lucht, W., Sykes, M. T., Thonicke, K., and Venevsky, S.: Evaluation of ecosystem dynamics, plant geography and terrestrial carbon cycling in the LPJ dynamic global vegetation model, Global Change Biol., 9, 161–185, doi:10.1046/j.1365-2486.2003.00569.x, 2003. 390

Tapley, B. D., Bettadpur, S., Ries, J. C., Thompson, P. F., and Watkins, M. M.: GRACE Measurements of Mass Variability in the Earth System, Science, 305, 503–506, doi:10.1126/science.1099192, 2004. 393

Walter, B. P., Heimann, M., and Matthews, E.: Modelling modern methane emissions from natural wetlands 1. Model description and results, J. Geophys. Res., 106, 34189–34206, 2001. 389

Wania, R., Ross, I., and Prentice, I. C.: Implementation and evaluation of a new methane model within a dynamic global vegetation model: LPJ-WHyMe v1.3.1, Geosci. Model Dev., 3, 565–584, doi:10.5194/gmd-3-565-2010, 2010. 390, 392, 396, 403

Whalen, S. C.: Biogeochemistry of Methane Exchange between Natural Wetlands and the Atmosphere, Environ. Eng. Sci., 22, 73–95, 2005. 389, 395

BGD
9, 387–409, 2012

Table 1. Model and observed decay constants for organic matter decomposition in anaerobic environments.

	Decay Constant (yr^{-1})	Study
Amazon Wetlands ($\overline{\phi}_{Amazon}$)	2.6–9.6[a] (median=5.9)	**This Study**: Top-down wetland CH_4 emission parameter optimization
Withered Leaves (35 °C)	4.0	**Miyajima et al. (1997)**: Decay constant from anaerobic tropical leaf CH_4 mineralisation
Wetland Macrophyte Decomposition	1.0–5.5	**Longhi et al. (2008)**[b]: Measured decomposition rates in Paluda di Ostiglia, Italy
Soil Carbon Pool (10 °C) Leaf Litter (10 °C) Root Exudates (10 °C)	0.001–0.03 0.35 13	**Wania et al. (2010)**: Bottom-up CH_4 Emissions from Northern Peatlands

[a] 68 % confidence interval
[b] Mass-loss decomposition rates

BGD
9, 387–409, 2012

Table 2. Estimates of total annual Amazon river basin wetland CH_4 emissions (Tg CH_4 yr^{-1}).

Study	Amazon Wetland CH_4 Emissions (Tg CH_4 yr^{-1})
Melack et al. (2004)	22
Fung et al. (1991)	5.3
Riley et al. (2011)	58.9[a]
Bloom et al. (2010)	20.0
This study	26.2 ± 9.8

[a] High tropical fluxes by Riley et al. (2011) are a result of anomalously high predicted net primary productivity in the Community Land Model (CLM version 4)

BGD
9, 387–409, 2012

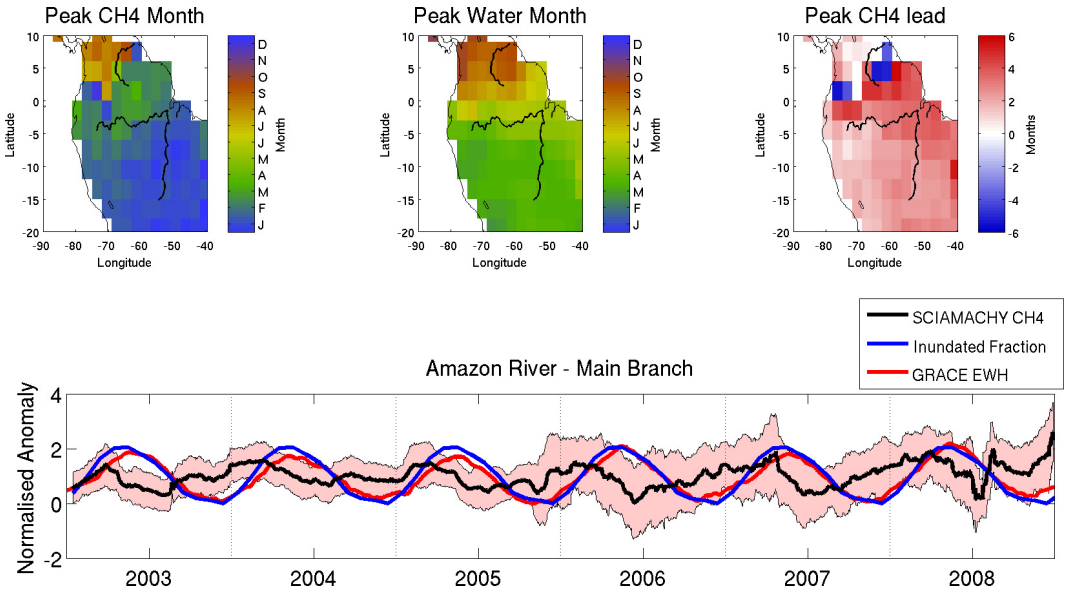

Fig. 1. Top: The timing (day of year) of peak CH_4 concentrations from SCIAMACHY (left), peak equivalent water height (EWH) from GRACE (middle), and the peak CH_4 concentration lead over tropical South America (right). Bottom: Normalised anomaly of GRACE EWH, mean flood fraction (Prigent et al., 2007) and mean CH_4 concentrations (including 1-standard deviation envelope) over the main branch of the Amazon river (0°–6° S, 40°–80° W).

BGD
9, 387–409, 2012

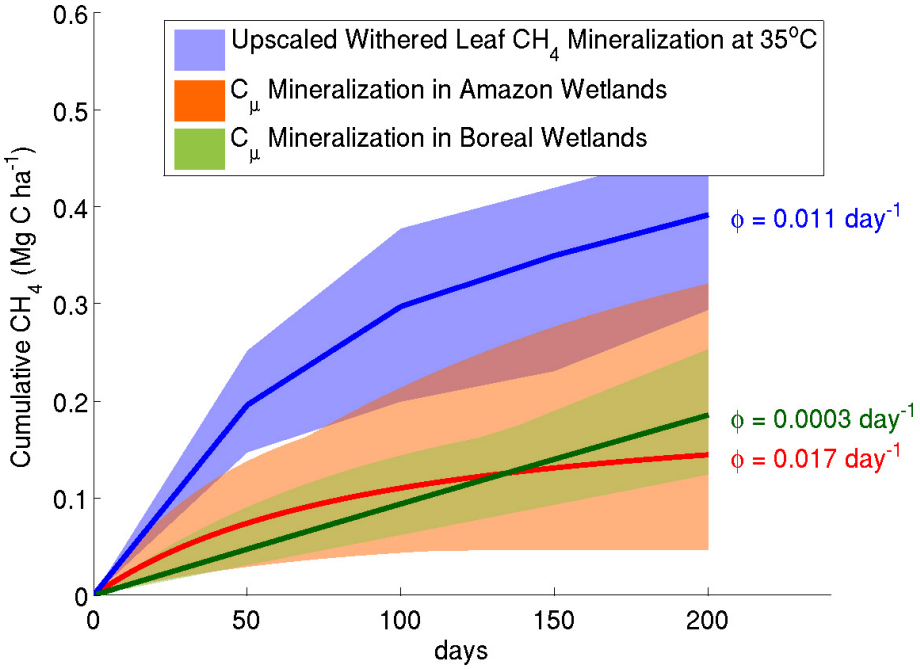

Fig. 2. Model and laboratory measurements of cumulative CH_4 emissions from withering leaves over a 200-day period. Blue: median and range of values from Miyajima et al. (1997). Red (green): median and 68 % confidence interval range of CH_4 emissions from the Amazon river basin (boreal wetland) from C_μ and $\overline{\phi}$ values when $N_\mu = 0$. A total litter stock of 17.5 Mg C ha^{-1} (Malhi et al., 2009) was used to upscale the Miyajima et al. (1997) CH_4 mineralisation rates.

BGD
9, 387–409, 2012

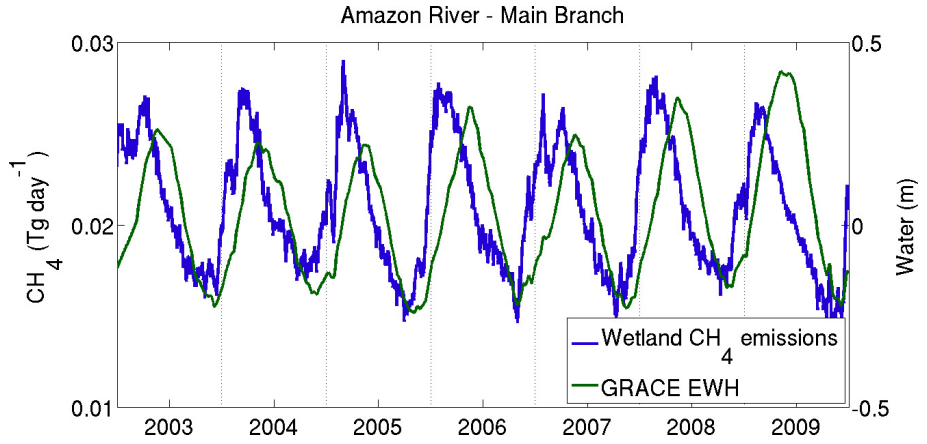

Fig. 3. Daily wetland CH_4 emissions for 2003–2009 (blue) and GRACE equivalent water height (green) over the central branch of the Amazon river (0°–6° S, 40°–80° W).

BGD
9, 387–409, 2012

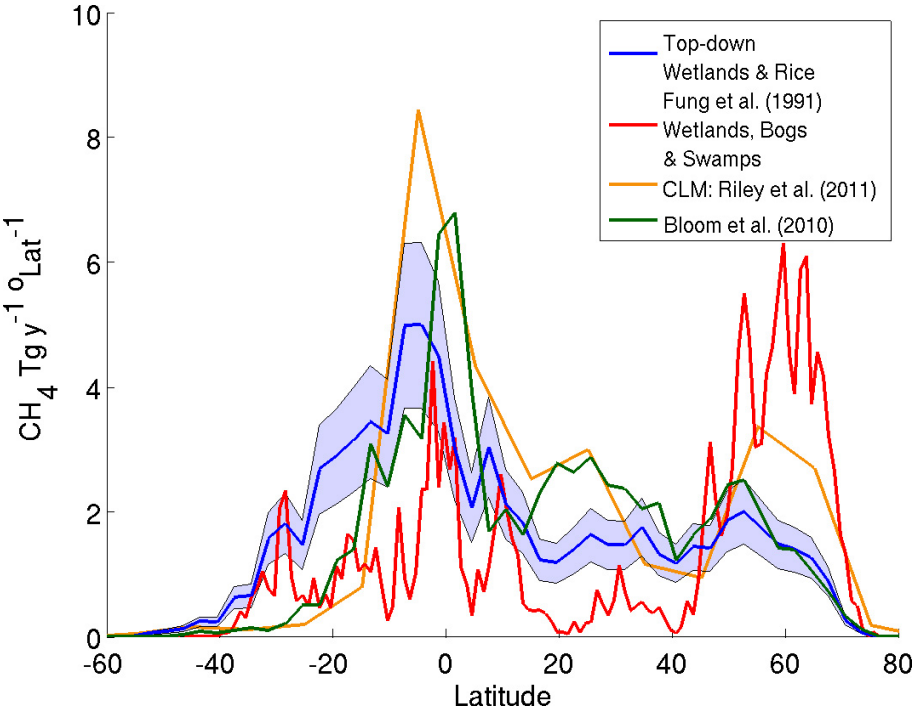

Fig. 4. Zonal profile of CH_4 emissions from wetlands and rice paddies: top-down approach (blue); Fung et al. (1991), wetlands only (red); Riley et al. (2011) wetland and rice paddy emissions (orange); Bloom et al. (2010) wetland and rice paddy CH_4 emissions (green). Riley et al. (2011) attribute their elevated tropical fluxes to anomalously high predicted net primary productivity in the Community Land Model (CLM version 4).

BGD
9, 387–409, 2012

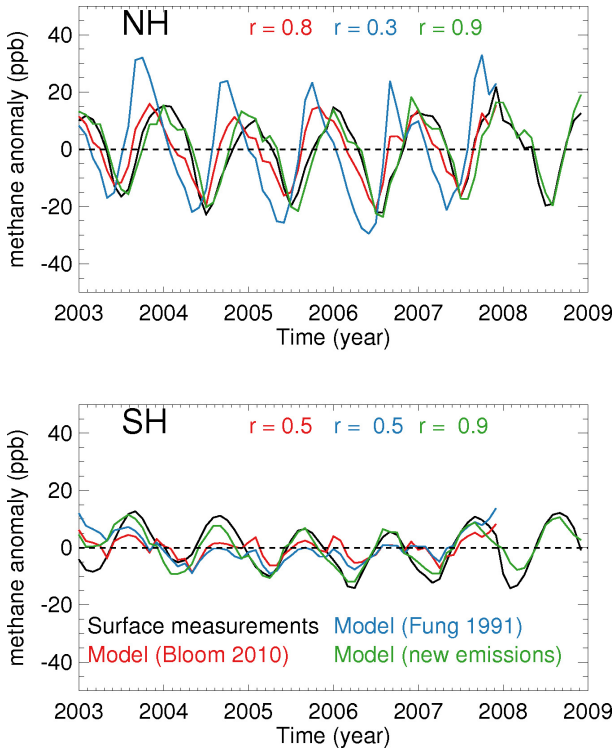

Fig. 5. Hemispheric mean observed and model methane anomalies from surface concentration measurements, 2003–2008. Surface concentration measurements (black) are from the GasLab, AGAGE and ESRL networks (Francey et al., 1996; Prinn et al., 2000; Cunnold et al., 2002; Dlugokencky et al., 2009). The GEOS-Chem global 3-D chemistry transport model (Fraser et al., 2011) is driven by wetland CH_4 emission estimates from Fung et al. (1991) (blue), Bloom et al. (2010) (red), and our new top-down approach (green).

BGD
9, 387–409, 2012